THERMOELECTRIC POWER SYSTEM FROM A LIQUID-FUELED-FIRED POROUS BURNER

By

AKMARUL HISHAM BIN SHAHARUDIN

(Matric No**:** 128926**)**

Supervisor

Dr. Khairil Faizi Mustafa

May 2019

Thesis submitted to Universiti Sains Malaysia
As partial fulfillment of the requirements
for the degree of
BACHELOR OF ENGINEERING (MECHANICAL ENGINEERING)

School of Mechanical Engineering
Engineering Campus
Universiti Sains Malaysia

DECLARATION FORM

This work has not previously been accepted in substance for any degree and is not being concurrently submitted in candidate for ny degree.

Signed…….....……(AKMARUL HISHAM SHAHARUDIN)

Date…….....

STATEMENT 1

This thesis is the result of my own investigation,except where otherwise stated. Other sources are acknowledge by giving explicit references. Bibliography/ references are appended.

Signed…….....……(AKMARUL HISHAM SHAHARUDIN)

Date…….....

STATEMENT 2

I hereby give consent for my thesis, if accepted, to be available for photocopying and for interlibrary loan, and for the title and summary to be made available outside organizations.

Signed…….....……(AKMARUL HISHAM SHAHARUDIN)

Date…….....

ACKNOWLEDGEMENT

I would like to express my gratitude towards the Most Gracious and the Most Merciful, Allah SWT for giving me the chance, granted with a good health and capability to finish this thesis.

I would like to address my debt and appreciation to the management of Universiti Sains Malaysia, for the opportunity to complete this four year course of mechanical engineering.

I would also like to express my gratitude towards Dr Khairil Faizi Mustafa, my dedicated supervisor who has been guiding me throughout this project. Greatest thanks for the opportunity given to undertake this final year project and for the endless help that was provided in finishing this project.

Also to the staffs of School of Mechanical Engineering for their fullest support. Their assistant and cooperation in making this project a success was much appreciated.

Not to forget, I would like to thanks all my friends and fellow families who have given me endless support and encouragement throughout this project. The continuous contribution either mentally, or physically, I'll accept with greatest thanks.

TABLE OF CONTENTS

ACKNOWLEDGEMENT ..... **iii**

TABLE OF CONTENTS ..... **iv**

LIST OF TABLES ..... **vi**

LIST OF FIGURES ..... **vii**

LIST OF SYMBOLS ..... **x**

LIST OF ABBREVIATIONS ..... **xi**

ABSTRAK ..... **xii**

ABSTRACT ..... **xiii**

CHAPTER 1 INTRODUCTION **1**

1.1 Research Background 1

1.2 Problem Statements 2

1.3 Objectives 2

1.4 Scope and Limitations 2

CHAPTER 2 LITERATURE REVIEW **4**

CHAPTER 3 METHODOLOGY **12**

3.1 Experiment Flow Chart 12

3.2 Procedure of Experiment 13

3.3 Combustion Calculation 16

3.4 Equipment and Apparatus 18

3.4.1 Multimeter 18

3.4.2 Thermal Imager 20

3.4.3 Anemometer 22

3.4.4 Thermoelectric Module 23

3.5 ANSYS Simulation. 23

CHAPTER 4 RESULT AND DISCUSSION..... 26

4.1 Experimental Results.....26

4.2 Simulation Results.....40

CHAPTER 5 CONCLUSION AND FUTURE RECOMMENDATIONS 46

5.1 Conclusion.....46

5.2 Recommendations for Future Research 47

5.2.1 Geometry modifications.....47

5.2.2 Blower installation. 48

REFERENCES..... 49

APPENDIX A: MEASURING DEVICE

APPENDIX B: SOLIDWORKS DRAWING OF COMBUSTION CHAMBER

APPENDIX C: SIMULATION SETTINGS

LIST OF TABLES

Page

Table 1 Result of temperature with various air fuel ratio 26

Table 2 Results of temperature with various equivalence ratio 32

Table 3 Results of equivalence ratio,Ø, voltage,V, current, I and power, P 36

Table 4 Simulation results.....44

LIST OF FIGURES

Page

Figure 2-1 Installation of both cold junction onto TE module 4

Figure 2-2 Installation of hot junction onto TE module 4

Figure 2-3 Plot of power output against ΔT 5

Figure 2-4 Voltage output against ΔT (right) 5

Figure 2-5 The overall overview of the combustion chamber 6

Figure 2-6 Images of flame shape and anchoring behaviour for combustor with different bead sizes 7

Figure 2-7 Stable operational envelopes for combustor with different bead sizes (bronze). 8

Figure 2-8 Temperature distributions at the combustor exit for different bead sizes. 9

Figure 2-9 Possible combinations for 50 modules gap height, flow rate to get maximum power 10

Figure 2-10 Gross power, net power, and maximum net power 10

Figure 2-11 Absolute gross power and maximum net power for different size of power generation system 11

Figure 3-1 Full setup of the experiment 13

Figure 3-2 Full setup of the experiment 14

Figure 3-3 Air flow inlet connection (a) and the coupling adapter (b) 14

Figure 3-4 Instek GDM-394 Multimeter 18

Figure 3-5 Fluke Ti-27 Infrared Thermal Imager 20

Figure 3-6 Digital Anemometer 22

Figure 3-7 Thermoelectric Module 23

Figure 3-8 SolidWorks model of the combustor chamber 24

Figure 3-9 Meshing options and settings. 24

Figure 3-10 Meshed model. 25

Figure 4-1 Captured images by thermal imager at air-fuel ratios of a=0.91, b=4.08 27

Figure 4-2 Captured images by thermal imager at air-fuel ratios of c=1.8, d=8.16 ..27

Figure 4-3 Captured images by thermal imager at air-fuel ratios of e=2.73, f=12.25 27

Figure 4-4 Captured images by thermal imager at air-fuel ratios of g=3.64, h=16.34 28

Figure 4-5 Captured images by thermal imager at air-fuel ratios of i=4.55, j=20.42 28

Figure 4-6 Graph of Temperature against Air -Fuel Ratio for $\dot{V}a$=10 l/min 29

Figure 4-7 Graph of Temperature against Air -Fuel Ratio for $\dot{V}a$=20 l/min 29

Figure 4-8 Graph of Temperature against Air -Fuel Ratio for $\dot{V}a$=30 l/min 30

Figure 4-9 Graph of Temperature against Air -Fuel Ratio for $\dot{V}a$=40 l/min 30

Figure 4-10 Graph of Temperature against Air -Fuel Ratio for $\dot{V}a$=50 l/min 31

Figure 4-11 Graph of Temperature against Equivalence Ratio for $\dot{V}a$= 10 l/min 33

Figure 4-12 Graph of Temperature against Equivalence Ratio for $\dot{V}a$= 20 l/min 33

Figure 4-13 Graph of Temperature against Equivalence Ratio for $\dot{V}a$= 30 l/min 34

Figure 4-14 Graph of Temperature against Equivalence Ratio for $\dot{V}a$= 40 l/min 34

Figure 4-15 Graph of Temperature against Equivalence Ratio for $\dot{V}a$= 50 l/min 35

Figure 4-16 Soot produce by rich combustions 36

Figure 4-17 Graph of current, I agaisnt voltage, V 37

Figure 4-18 Graph of power, P against equivalence ratio, Ø.....38

Figure 4-19 Combustion that occur at fuel outlet. 40

Figure 4-20 Velocity profile of Ø=0.81285 combustion 40

Figure 4-21 Temperature contour of Ø=0.81285 combustion 41

Figure 4-22 External wall of Ø=0.81285 combustion 41
Figure 4-23 Velocity profile of Ø=1.01606 combustion 41
Figure 4-24 Temperature contour of Ø=1.01606 combustion 42
Figure 4-25 External wall of Ø=1.01606 combustion 42
Figure 4-26 Velocity profile of Ø=1.35475 combustion 42
Figure 4-27 Temperature contour of Ø=1.35475 combustion 43
Figure 4-28 External wall of Ø=1.35475 combustion 43

LIST OF SYMBOLS

K	Kelvin
°C	Degree Celsius
°F	Degree Fahrenheit
V	Voltage, Volt
I	Current, Ampere
W	Watt
P	Power
Ω	Ohm
g	Gram
s	Second
Hz	Hertz
Ø	Equivalence Ratio
m	Meter

LIST OF ABBREVIATIONS

TE	Thermoelectric
TEGs	Thermoelectric Generators
CO	Carbon Monoxide
CO_2	Carbon Dioxide
NO_2	Nitrogen Oxides
H	Hydrogen
C	Carbon
N_2	Nitrogen Gas
O_2	Oxygen Gas
H_2O	Water
A/F ratio	Air Fuel Ratio
F/A ratio	Fuel Air Ratio
A/F stoichiometry	Stoichiometry Air Fuel Ratio
T	Temperature

SISTEM PENJANAAN KUASA TERMOELEKTRIK BEDASARKAN PEMBAKARAN BAHAN API CECAIR MELALUI MEDIA BERLIANG

ABSTRAK

Projek ini membentangkan sistem penjanaan kuasa termoelektrik yang menggunakan bahan api cecair yang dinyalakan melalui media berliang. Tujuan kajian ini dijalankan adalah untuk menguji kebolehan modul termoelektrik terbabit untuk menjana tenaga elektrik berdasarkan haba yang dihasilkan oleh pembakaran bahan api cecair. Sistem ini menggunakan kerosin sebagai bahan api, dibakar dengan pelbagai nisbah setara bahan api−udara diantara Ø = 0.813 hingga Ø = 18.227. Suhu hasil dari pembakaran disukat menggunakan alat pengimejan haba, manakala, kuasa yang dijana oleh modul termoelektrik disukat menggunakan multimeter dan dikenalpasti bahawa di nisbah kesetaraan bersamaan dengan satu, modul termoelektrik mampu menjana kuasa tertinggi, iaitu P = 1.056 W dengan purata suhu, T = 437.25 °C. Kuasa yang dijana di kawasan kekurangan bahan api dengan nilai Ø = 0.183 ialah P = 0.602 W dengan purata suhu T = 425.04 °C. Manakala kuasa yang dijana di kawasan yang kaya bahan api dengan nilai Ø = 2.036 ialah P = 0.293 W dengan purata suhu T = 500.62 °C. Ianya telah dikenal pasti bahawa, pada nilai Ø = 1, kuasa yang mampu dijana adalah maksima, manakala dengan nilai Ø yang lebih besar atau kecil, kuasa yang dijana akan semakin berkurangan. Walaubagaimanapun, suhu yang disukat didapati semakin meningkat dengan meningkatnya tempoh waktu pembakaran. Justeru, prestasi sistem penjanaan kuasa termoelektrik telah dinilai dan diperolehi di kedua belah kawasan kekurangan dan kaya dengan bahan api.

THERMOELECTRIC POWER SYSTEM FROM A LIQUID-FUELED-FIRED POROUS BURNER

ABSTRACT

This project presents a set up of a thermoelectric power system that uses liquid fuel, fired through a porous media burner. The aim of the study is to evaluate the capability of the thermoelectric module to generate electricity based on the heat produce by the combustion of the liquid fuel. The system uses kerosene as a fuel, combust with variety of equivalence ratio between Ø = 0.813 to Ø = 18.227. Heat as the product of the combustion is measured using a thermal imager device, and the power generated by the thermoelectric module is measured using multimeter and it is found out that at an equivalence ratio equal to one, the module generate the highest power, where P = 1.056 W with average temperature of T = 437.25 °C. The power generated at fuel-lean region with Ø = 0.813 is P = 0.602 W with average temperature T = 425.04 °C. Whereas the power generated at fuel-rich region with Ø = 2.036 is P = 0.293 W with average temperature of T = 500.62 °C. It is found out that the highest power generated can be obtained at Ø = 1, and the power generated decrease with lower or higher value of Ø. However, the measured temperature is found out to increase with increasing period of combustion. Hence, the performance of the thermoelectric power generating system is evaluated and achieve at both fuel-lean and fuel-rich region.

CHAPTER 1
INTRODUCTION

1.1 Research Background

Liquid fuel combustion has been widely used for transportation and power generation applications because of their high fuel efficiency. However, the process of combustion produces large amount of heat that is not being used by the system. Taking the heat produce by an automobile as reference, statistically, 40% of the heat generated is release to the atmosphere through the exhaust (He, Wang, & Yang, 2016) and 6% of these heat can be converted into electrical power resulting in about 10% reduction of fuel consumptions (Vázquez, Sanz-Bobi, Palacios, & Arenas, 2002). This is made possible with the use of thermoelectric (TE) devices where electrical energy is generated when heat flows through the semiconductor material due to the temperature gradient between the hot and cold junctions (Mustafa, Abdullah, Abdullah, & Sopian, 2017).

In general, Thermoelectric (TE) module is a device that is capable to produce electricity due to the temperature difference between the hot and cold junction(Zheng, Liu, Yan, & Wang, 2014). TE modules converts thermal energy directly into electrical energy(Qiu & Hayden, 2012). Nevertheless, the efficiency of TE devices are relatively low. The efficiencies however depends on various methods of fuel-air mixing processes, fuel-air equivalence ratio, and thermal and combustion characteristics. Among these, fuel-air mixture role is significant for TE power devices(Mustafa et al., 2017).

1.2 Problem Statements

The thermoelectric (TE) module main purpose is to generate electric energy by converting heat energy into electrical energy. Therefore, the main focused of the present paper is to investigate the generated power output of the TE system via liquid fuel combustion through porous burner. The primary aim of the study is to understand the influence of air-fuel equivalence ratios towards the performance of the TE system. Difference air-fuel equivalence ratio would lead to either fuel-lean or fuel-rich combustion. Hence, by knowing the optimum electricity produce by the TE module in either condition, we can assume which is the best for the TE module to operate.

1.3 Objectives

1. To determine the heat flow on the combustion chamber.
2. To evaluate the effect of porous burner and air-fuel mix ratios.
3. To measure the electrical energy generated by the thermoelectric system.

1.4 Scope and Limitations

There are several scope of work to accomplish the objectives of this paper. The parameter of this work started with studying the design of previously fabricated combustion chamber as to understand how would the combustion chamber operate and hence prepare the combustion chamber for the experiments. Then, from the combustion of the fuels, flame changes and heat produced by the combustion will be investigated in various value of equivalence ratios. This is to evaluate the effects of equivalence ratios towards the flame formations and heat production by the combustions.

Next is to simulate the combustion process occurred in the combustion chamber as to study the heat flow in the combustion chamber, and approximate

temperature gradient of the combustions. Then, the results will be compared with the experimental results.

Last but not least, the thermoelectric module will be tested with the combustions of the fuels. The results of voltage, current and power generated by the thermoelectric module will be evaluated.

CHAPTER 2
LITERATURE REVIEW

Based on the research done by (Liu & Zhong Li, 2013) the system could achieve maximum power output with varying temperature difference, ΔT. In their paper, water–cooling method is proposed to keep the temperature difference between the hot and cold junction. Forty-eight aluminium cooling plates are used as thermal spreader to provide uniform temperature and pressure distribution across the TE module. Whereas for the hot junction, electric heating rod is chosen, heating a flat structure with conducting oil filling the cavity of the structure. Figure 2-1 and Figure 2-2 shows the layout of both cold and hot junction.

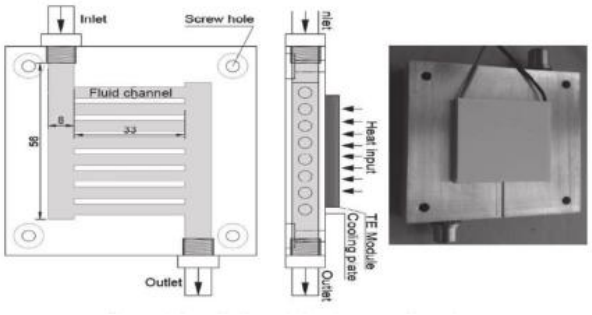

Figure 2-1 Installation of both cold junction onto TE module

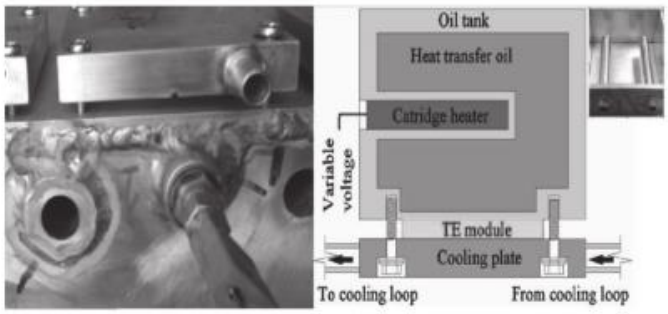

Figure 2-2 Installation of hot junction onto TE module

Based on their experiment, a trend of incresing value of power output with respect to increasing value of ΔT is observed. Figure 2-3 and Figure 2-4 shows the trend of power output and voltage output with increasing value of ΔT.

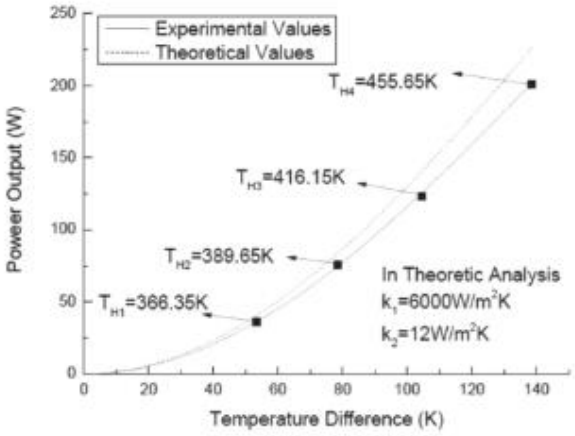

Figure 2-3 Plot of power output against ΔT

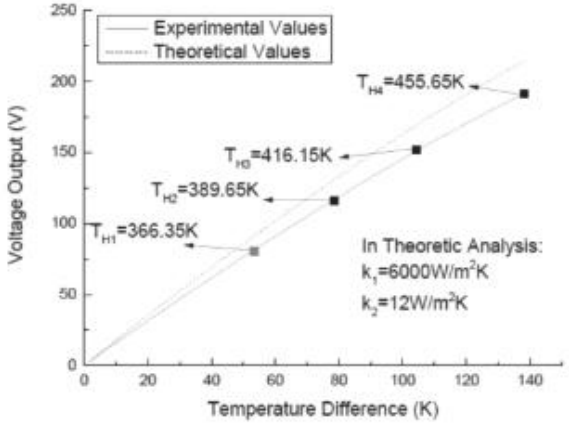

Figure 2-4 Voltage output against ΔT (right)

However, at high temperatures, there are deviations between predicted value of power output from the TE module. This is due to the fact that not all heat from the hot side is absorbed by the TE module. There is a limit to which amount of heat that is capable to be absorbed by the TE module. A suggestion to improve this condition is by

installing multiple TE module across the hot and cold junction as to improve the amount of heat being absorbed rather than radiates into waste.

Whereas from the reasearch done by (Xiao, Qiu, Gou, & Ou, 2013) a research was done to investigate several condition that may increase the output of thermoelectric generator, TEG. In their research, they developed a flameless catalytic combustion-based TEG. Natural gas was used for the combustion inside the chamber. In order to establish appropriate temperature difference, three large heat sinks was used to surround the chamber, which the cold sides of the TE module are fixed. Figure 2-5 shows the layout of the combustion chamber.

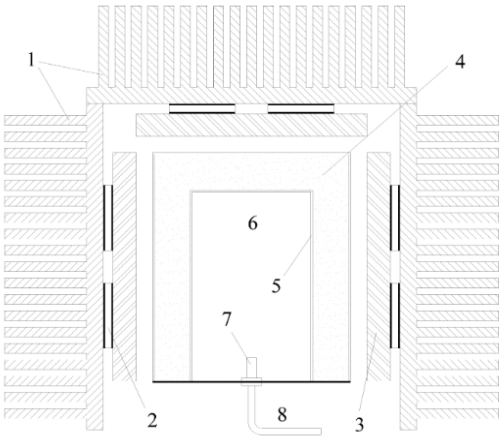

1-Heat sink 2-Thermoelectric module 3-Thermal plate 4-Asbestos layer
5-Porous metal plate (catalytic reaction layer) 6-Combustion chamber
7-Nozzle 8-Natural gas tube

Figure 2-5 The overall overview of the combustion chamber

It was found that the TEG can perform better with uniform heat distribution towards the TE module. In the test, indirect heat from the combustion is used. The TE module has the advantage from the natural gas combustion inside the chamber. This has left the system with nonuniformed heat distribution. Thus, by having a direct combustion heat to be absorbed by the TE module, lower time to achieve stability and uniform heat distribution across the TE module can be obtained.

In other work that have been done by (Li, Chao, & Dunn-Rankin, 2008) a stable flame of combustion can be obtained by using a porous media burner. In their experiment, they tested the combustion of fuel in porous burner with different material and sizes. Based on their findings, different type of material produces stable flame at different air flow. This is due to the thermal conductivity and thermal diffusivity of the material. The thermal conductivity of the porous medium would influenced fuel vaporization rate, hence effects the combustion phenomena in the chamber. With different air flow rate and bead sizes, the flame of the fuel combustion doesn't change drastically. Figure 2-6 shows the stability of flames under different value of air flow rate and bead sizes.

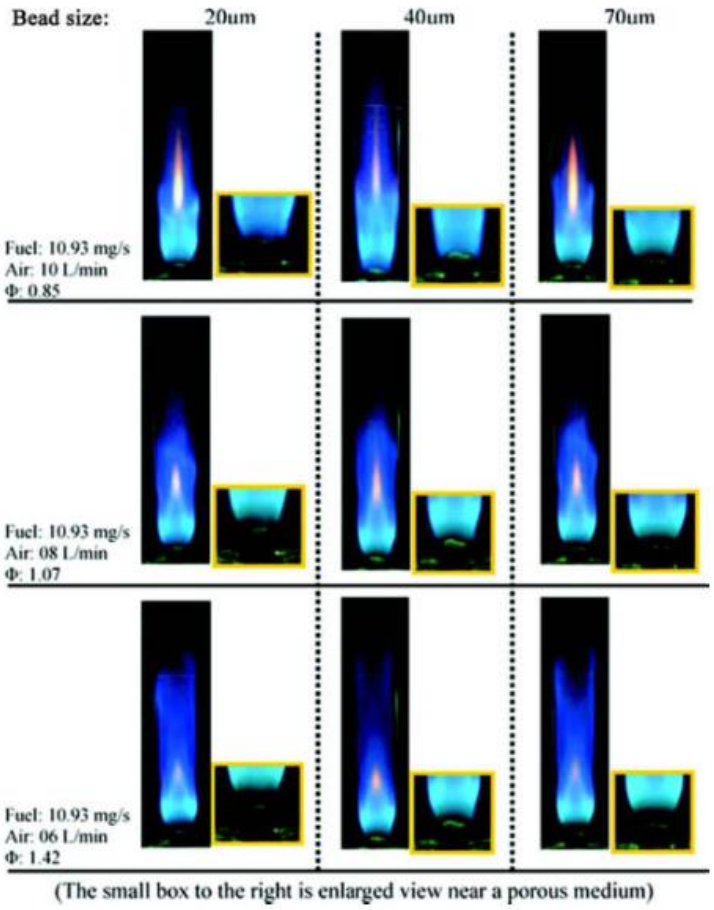

Figure 2-6 Images of flame shape and anchoring behaviour for combustor with different bead sizes

A smaller stable operation range was achieved with larger bead sizes. This is due to the relatively lower thermal conductivity and thermal mass, hence the ability to absorb heat from the flame for fuel vaporization is lower compared to smaller beat sizes porous medium. Moreover, the fuel spread for larger beat size is dominated by external flow rather than capillarity. This cause the larger bead size combustor to be more sensitive towards external pertubation. Figure 2-7 shows that larger bead size medium have smaller stable operational range whereas Figure 2-8 shows the exit temperature distribution of combustor with difference bead size and air flow rate. It shows that the heat release is dependant on the bead sizes.

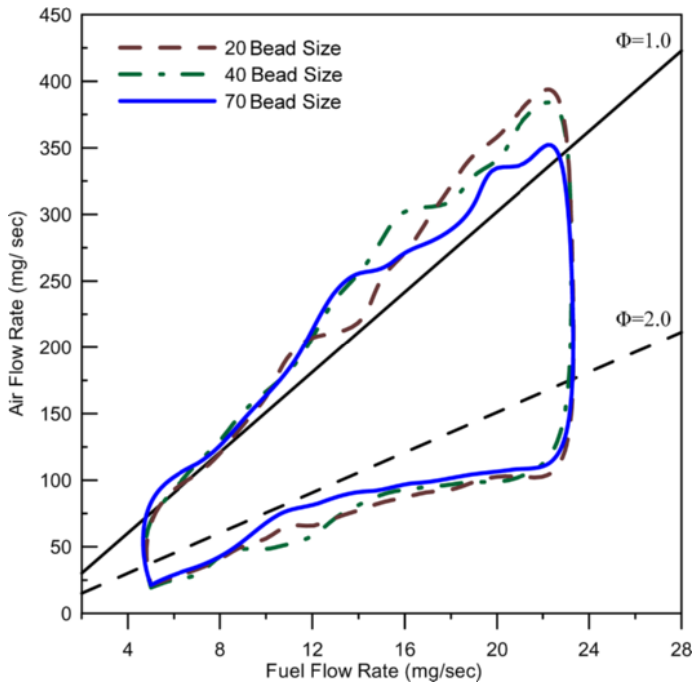

Figure 2-7 Stable operational envelopes for combustor with different bead sizes (bronze).

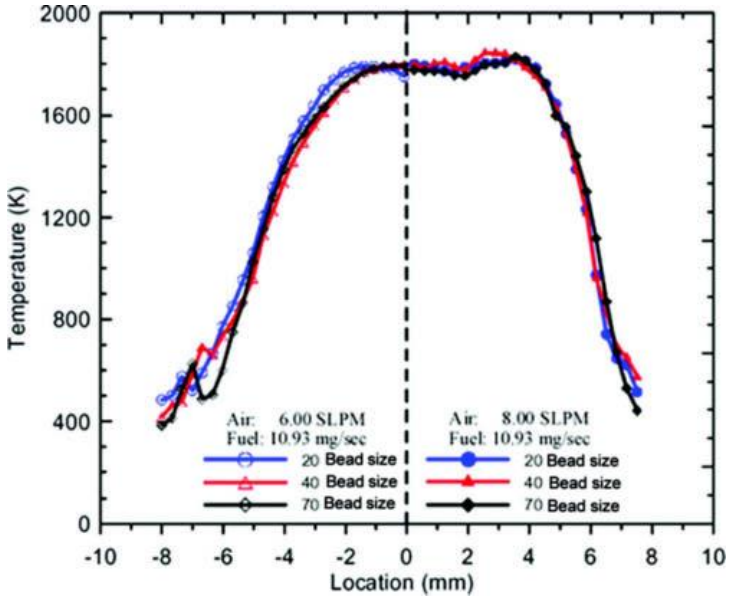

Figure 2-8 Temperature distributions at the combustor exit for different bead sizes.

Next, from the work done by (Rana, Date, Iqbal, & Akbarzadeh, 2019), they have simulate an optimization of a thermoelectric generator power system. Their model uses 50 TEG modules, placed in between a hot water channel and a cold water channel. The TEG properties and waste heat properties are set as the fixed input. Whereas the variable input consist of the flow rate, gap height, and also the length and width of the heat exchanger. Their proposed model is capable to predict gross power, nett power, and pumping power for all operating conditions. Their simulation runs with hot side temperature, T_h = 90°C and the cold side temperature of of T_c = 15°C, flow rate varies from 1 l/min to 300 l/min and gap height of 1 mm to 3 mm. Thermal resistance and efficiency of the TEG modules is considered as 0.72 (°C/W) and 1.91% respectively. Figure 2-9 shows the maximum net power, respective gap height and flow rate.

Length (m)	Width (m)	Gap height (mm)	Flow rate (L/min)	Net Power (W)
2	0.04	15	46	76.15
1	0.08	9	56	77.97
0.4	0.2	6	92	78.79
0.2	0.4	5	153	78.97
0.08	1	4	300	79.02
0.04	2	2	289	78.66

Figure 2-9 Possible combinations for 50 modules gap height, flow rate to get maximum power

The maximum power output of 79.02 W is obtained at the combination of 0.08m long, 1m wide, 4mm gap height and 300 l/min flow rate. Figure 2-10 below shows the plot of power generated by the TEG modules.

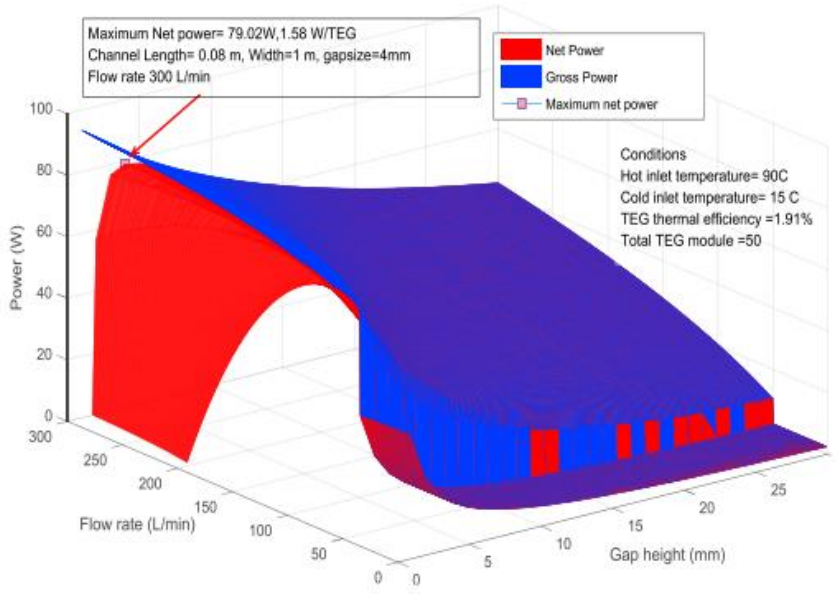

Figure 2-10 Gross power, net power, and maximum net power

Whereas for the effect of number of modules on power generated, a number of simulations have been done using 50, 100, 500, 1000, 2000, 5000, and 10000 combinations of TEG module. The condition for this simulation is that the flow rate is considered 6 times to the number of TEG module, varied gap height of 1mm to 30mm, T_h = 90°C, T_c = 15°C, TEG efficiency of 1.91% and thermal resistance of 0.72 °C/W.

The absolute gross power and maximum net power per module of different number of TEG sets used is shown in Figure 2-11 below.

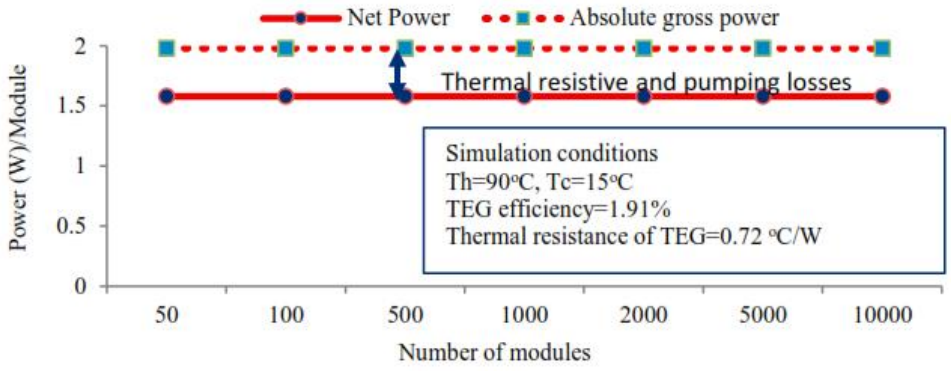

Figure 2-11 Absolute gross power and maximum net power for different size of power generation system

Figure 2-11 also shows the power losses due to convective and conductive thermal resistance and pumping power losses. From this work, the theoretical model has shown that combinations of varying parameter would produce various amount of generated power. However, this work role with the temperature difference between a channel of hot water and a channel of cold water only.

CHAPTER 3
METHODOLOGY

3.1 Experiment Flow Chart

‘

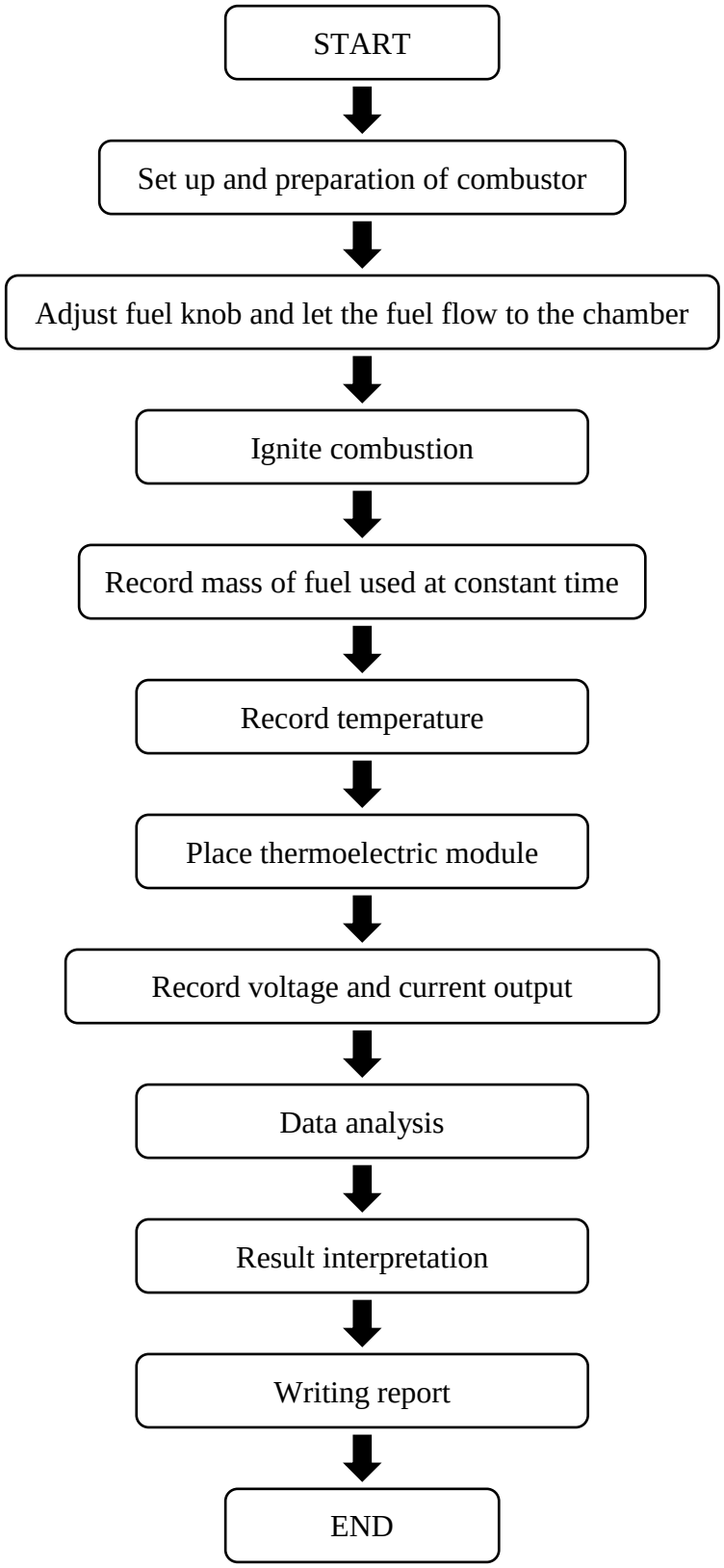

From the flow chart, the full set up of the combustor is firstly done. The flow of combustion start off with air being supplied to the chamber, followed by the fuel that is gravitationally fed onto the porous media burner that is placed in the center of the combustor. The combustion is then ignited by using lighters that provide initial heat for the combustion to occur. The temperature of the porous media burner is recorded using the thermal imager. All result are tabulated.

3.2 Procedure of Experiment

First, the required material and components were prepared. This includes the air flow supply, anemometer, combustion chamber, liquid kerosene, thermal imager, multimeter and thermoelectric module.

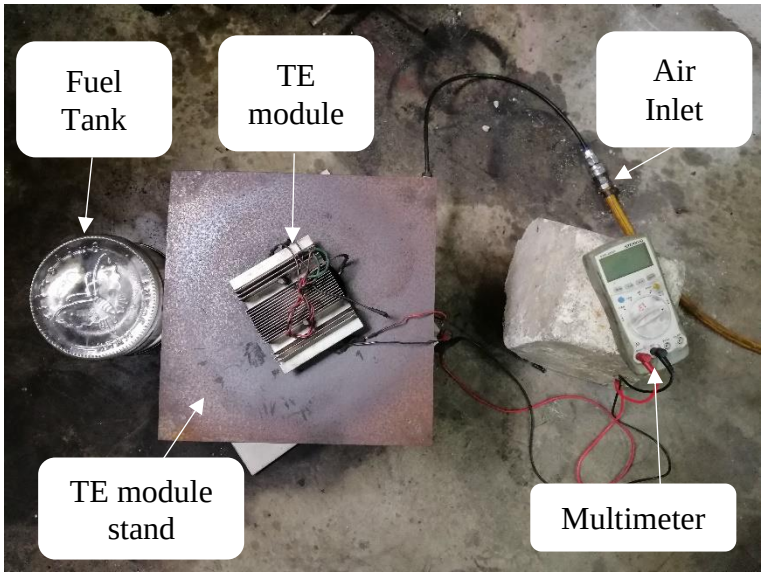

Figure 3-1 Full setup of the experiment

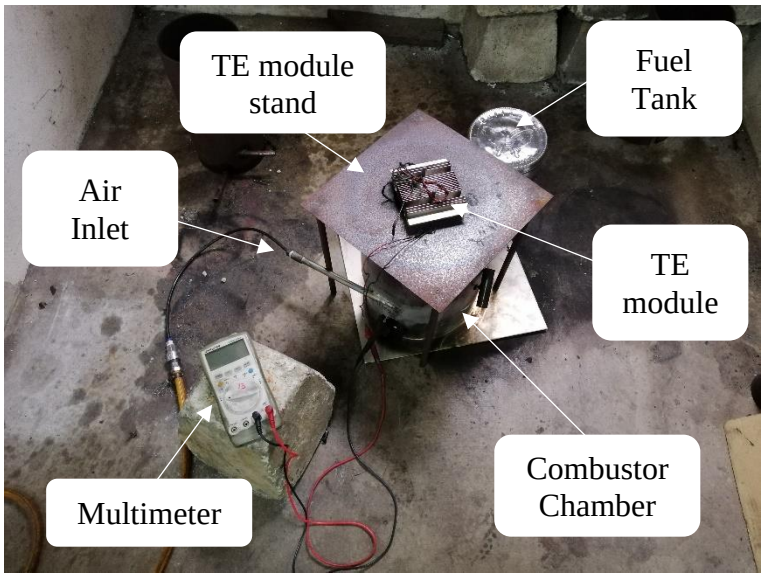

Figure 3-2 Full setup of the experiment

The air flow was controlled by adjusting the velocity of air. Anemometer was used to read the velocity of the compressed air. The outlet from the compressed air supply was connected to the air flow inlet in the combuster via the coupling adapter.

Figure 3-3 Air flow inlet connection (a) and the coupling adapter (b)

Then fuel was weight to measure the initial mass of the fuel before the combustion. The fuel was then poured into the fuel tank. The fuel was fed into the combustion chamber via a throttle. The throttle was adjusted to release the desired amount of fuel into the combustion chamber.

Next, the combustion was ignited inside the chamber. A lighter and a piece of paper was used to introduced heat to the porous media burner. Once the combustion started, the chamber was let to burn for around five to ten minutes. The time for combustion was measured and recorded. Then, the thermal imager was used to measure the temperature at the center of the porous media burner. Data of the temperature of the porous media burner was recorded.

Then the thermoelectric stand was placed on top of the chamber, followed by the thermoelectric module that was placed on top of the stand. The sets of thermoelectric module was connected in series where the end wire was connected to a multimeter. The red end wire was connected to the red probe and the black end wire was connected to the black probe. The voltage and current produce by the thermoelectric module was measured using the multimeter and recorded.

The steps were repeated using various values of air flow rate and fuel flow rate. The air flow rate used was 10, 20, 30, 40, and 50 l/min whereas the fuel flow rate was adjusted for 5 types of openings. This combination of fuel openings were repeated for all five type of air flow rate used.

The data obtained from the experiment were tabulated and analyse. Power generated by the thermoelectric module was calculated by the equation of power, P = VxI, where V is voltage and I is current. Several graphs were then plotted which include,Temperature, T against Air Fuel Ratio, $A/F_{ratio,}$ Temperature,T against Equivalence Ratio, Ø, Current, I agaisnt Voltage, V and Power, P against Equivalence Ratio, Ø.

3.3 Combustion Calculation

Most of the liquid fuels available are the combinations of hydrocarbons with varying number of carbon and hydrogens atoms. Generally, liquid fuel hydrocarbons is summarize as a single hydrocarbon with an empirical formula of CxHy. Most commonly used hydrocarbon includes gasoline, diesel, and kerosene. In this experiment, kerosene is used and a molecular number of $C_{12}H_{23}$ is assumed. Kerosene is obtained via fractional distillation of petroleum between 150 and 275°C, which produce clear liquid with low viscosity composed of carbon chains typically between 10 to 16 carbon atoms per molecule.

When a liquid fuel is reacted with oxygen, heat is generated as a product of the reaction and this heat can be harvested to be used for various purposes. This process is known as combustion. When liquid fuel reacts with pure oxygen, it gives out products and heat. Thus, the process will always be exothermic as heat is release from the reaction. The general chemical reaction of liquid fuel reacting with pure oxygen undergoing combustion can be written as:

$$Fuel + O_2 \rightarrow Products + Heat$$

The products of the combustion consists of carbon dioxide, CO_2 and water, H_2O

Wheras for kerosene,

$$4C_{12}H_{23} + 71O_2 \rightarrow 48CO_2 + 46H_2O$$

The amount of air that is used to complete the combustion is known as stoichiometry, or theoretical air. Stoichiometry air is used completely in a combustion process without excess air or excess fuel in the end.

Whereas for an incomplete combustion, there are either excess air, or excess of fuels. The condition where air is in excess is referred as lean combustion and the

condition where fuel is in excess is known as rich combustion. The general combustion of liquid fuel with pure air can be written as:

$$C_xH_y + v_{O_2}(O_2 + 3.76N_2) \rightarrow v_{CO_2}CO_2 + v_{H_2O}H_2O + v_{N_2}N_2$$

Balancing the atoms as to achieve a complete combustion, or also known as clean combustion, would results in obtaining the amount of theoretical air for the combustion. The outcome value of the coefficients is known as stoichiometric coefficients. For stoichiometry balancing,

C: $V_{CO2} = x$

H: $2(V_{H2O}) = y$

N_2: $V_{N2} = 3.76(V_{O2})$

O_2:$V_{O2} = V_{CO2}+V_{H2O}$

$2 = x+y/4$

Thus the total number of moles of air for 1 mole of fuel becomes

$n_{air} = V_{O2}(4.76) = 4.76(x+y/4)$

In real application, the parameters used to obtained either lean or rich combustion are either air fuel ratios, A/F_{ratio} or the fuel air ratio, F/A_{ratio}. These ratios can normally be controlled in an application. Both air fuel ratio and fuel air ratio are defined as,

$$A/F_{ratio} = \frac{\dot{m}_a}{\dot{m}_f}$$

$$F/A_{ratio} = \frac{\dot{m}_f}{\dot{m}_a}$$

In terms of mole,

$$A/F_{ratio} = \frac{n_a}{n_f}$$

$$F/A_{ratio} = \frac{n_f}{n_a}$$

From these A/F_{ratio}, the equivalence ratio can be found. The equivalence ratio can be used to identify either lean or rich combustion occurred. The equivalence ratio is given as,

$$Equivalence\ Ratio, \emptyset = \frac{A/F_{stoichiometry}}{A/F_{actual}}$$

$A/F_{stoichiometry}$ is the chemically correct air fuel ratios that would satisfy a complete combustion. Hence, for Ø=1, the combustion is said to be in stoichiometry, where no excess air or fuel is present. For Ø<1, the combustion is in the lean region, with exces air, and for Ø>1, the combustion is in the rich region, where there are excess of fuels.

3.4 Equipment and Apparatus

In this section, list of equipment used in the experiment was shown with their specifications.

3.4.1 Multimeter

Figure 3-4 Instek GDM-394 Multimeter

DC VOLTAGE	
Range	400mV, 4V, 40V, 400V, 1000V
Best Accuracy	±(0.8%rdg + 1digit)
Input Impedance	10MΩ
AC VOLTAGE (50Hz ~ 400Hz)	
Range	4V, 40V, 400V, 750V
Best Accuracy	±(1%rdg + 5 digits)
Input Impedance	10M Ω
DC CURRENT	
Range	400uA, 4mA, 40mA, 400mA, 4A, 10A
Best Accuracy	±(1.5%rdg + 5 digits)
RESISTANCE	
Range	400 Ω ~ 40M Ω 6 ranges
Best Accuracy	±(1%rdg + 2 digits)
GENERAL	
Continuity Beeper	Buzzer sounds if conductance less than 70 Ω
Open Voltage Diode Test	3.0V typical
Special Function	Duty cycle, Auto Ranging
Display	3999 counts
Power Source	Single 9V battery (6F22)
Accessories	Test leads, Instruction manual, battery
Dimensions & Weight	85(W) x 177(H) x 40(D) mm , Approx.330g
CAPACITANCE	
Range	40nF, 400nF, 4 μ F, 40 μ F,100uF
Best Accuracy	±(3%rdg + 5 digits)
FREQUENCY	
Range	10Hz ~ 10MHz
Best Accuracy	±(0.1%rdg + 3digits)
Temperature(°C)	
Range	-40°C~1000°C
Best Accuracy	±1%+3

3.4.2 Thermal Imager

Figure 3-5 Fluke Ti-27 Infrared Thermal Imager

Temperature	
Temperature measurement range (not calibrated below -10°C)	-20°C to +600°C (-4°F to +1112°F)
Temperature measurement accuracy	± 2°C or 2% (at 25°C nominal, whichever is greater)
On-screen emissivity correction	Yes
On-screen reflected background temperature compensation	Yes
On-screen transmission correction	Yes
General Specifications	
Operating temperature	-10°C to +50°C (14°F to 122°F)
Storage temperature	-20°C to +50°C (-4°F to 122°F) without batteries
Relative humidity	10% to 95% non-condensing
Display	9.1 cm (3.7 in) diagonal landscape color VGA (640 x 480) LCD with backlight and clear protective cover
Controls and adjustments	User selectable temperature scale (°C/°F)
	Language selection
	Time/Date set
	Emissivity selection
	Reflected background temperature compensation
	Transmission correction
	User selectable hot spot and cold spot, and center point on the image (other custom markers and shapes in SmartView® software)

	High temperature color alarm
	User selectable backlight: “Full Bright or "Auto"
	Information display preference
Software	SmartView® full analysis and reporting software included
Batteries	Two lithium ion rechargeable smart battery packs with five-segment LED display to show charge level
Battery life	Four+ hours continuous use per battery pack (assumes 50% brightness of LCD)
Battery charge time	2.5 hours to full charge
AC battery charging	Two-bay AC battery charger (110 V AC to 220 V AC, 50/60 Hz) (included), or in-imager charging. AC mains adapters included. Optional 12 V automotive charging adapter.
AC operation	AC operation with included power supply (110 V AC to 220 V AC, 50/60 Hz). AC mains adapters included.
Power saving	Sleep mode activated after five minutes of inactivity, automatic power off after 30 minutes of inactivity
Safety standards	CSA (US and CAN): C22.2 No. 61010-1-04, UL: UL STD 61010-1 (2nd Edition), ISA: 82.02.01
Electromagnetic compatibility	Meets all applicable requirements in EN61326-1:2006
C Tick	IEC/EN 61326-1
US FCC	CFR 47, Part 15 Class B
Vibration	0.03 g2/Hz (3.8 grms), IEC 68-2-6
Shock	25 g, IEC 68-2-29
Drop	2 m (6.5 ft) with standard lens
Dimensions (H x W x L)	27.7 x 12.2 x 17.0 cm (10.9 x 4.8 x 6.7 in)
Weight (battery included)	1.05 kg (2.3 lb)
Enclosure rating	IP54 (protected against dust, limited ingress; protection against water spray from all directions)
Warranty	Two-years (standard)
Recommended calibration cycle	Two-years (assumes normal operation and normal aging)
Supported languages	Czech, English, Finnish, French, German, Italian, Japanese, Korean, Polish, Portuguese, Russian, Simplified Chinese, Spanish, Swedish, Traditional Chinese, and Turkish

3.4.3 Anemometer

Figure 3-6 Digital Anemometer

Air Velocity	
Range	0 - 30m/s, 0 - 90km/h, 0 - 5860ft/min, 0 - 65mph, 0 - 55Knots.
Resolution	0.1m/s, 0.3km/h, 19ft/min, 0.2mph, 0.2Knots
Threshold	0.1m/s, 0.3km/h, 39ft/min, 0.2mph, 0.1Knots.
Accuracy	+/- 5%.
Air Temperature	
Range	-10°C ~ +45°C, 14°F~ 113°F.
Resolution	0.2°F, 0.36°F
Accuracy	±2°C, ±3.6°F
Thermometer	NTC Thermometer.
Operating Temperature	-10°C ~ +45°C (14°F~ 113°F)
Operating Humidity	Less than or equal to 90% RH
Storage Temperature	-40°C ~ +60°C, -40°F ~140°F
Current Consumption	About 3mA.
Powered by	3V CR2032 Battery
Dimensions	10.7cm x 4.5cm x 2.1cm - 4.21inch x 1.77inch x 0.83inch.

3.4.4 Thermoelectric Module

Figure 3-7 Thermoelectric Module

A Thermoelectric (TE) module is an electronic component which based on semiconductor that function either by using electricity or to produce electricity. By consuming electricity, a thermoelectric module is able to move heat from a hot junction to the cold juntion of the semiconductor. In reverse, the thermoelectric module can produce electricity by using heat difference between the hot and cold junction. This occur due to the free electron that contains within the p and n junction of the module. Upon receiving heat at the hot junction, these electron will travel to the opposite site of the cold junction. These movement of electrons generate electricity thorughout the thermoelectric module. In this experiment, the thermoelectric module is couple with heat sink that consists of fins. This is to obtained the maximum heat difference between the hot and cold junction.

3.5 ANSYS Simulation.

Overall, simulating the combustion involves the process of creating geometry, meshing up the geometry, setup of the combustion processes, run calculation and finally interpretation of the results obtained. In this work, ANSYS Fluent was used as

it was compatible for computational fluid dynamics calculations. ANSYS program that was used was the ANSYS 2019 R1 Academic Version.

First step taken was to import the geometry into ANSYS. The geometry of the combustor model was design in the SolidWorks program.

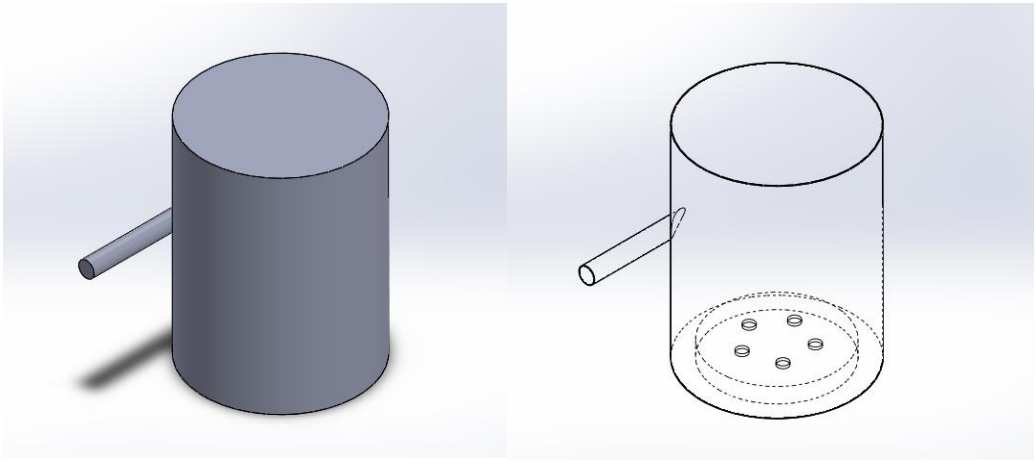

Figure 3-8 SolidWorks model of the combustor chamber

Next, the model was meshed. Meshing was done with the settings show in Figure 3-9 below. High smoothing option for the mesh in the quality section was also selected.

Defaults	
Physics Preference	CFD
Solver Preference	Fluent
Element Order	Linear
Element Size	Default (3.2016e-002 m)
Export Format	Standard
Export Preview Surface Mesh	No
Sizing	
Use Adaptive Sizing	No
Growth Rate	Default (1.2)
Max Size	Default (6.4031e-002 m)
Mesh Defeaturing	Yes
Defeature Size	Default (1.6008e-004 m)
Capture Curvature	Yes
Curvature Min Size	Default (3.2016e-004 m)
Curvature Normal Angle	Default (18.0°)
Capture Proximity	No
Bounding Box Diagonal	0.64031 m
Average Surface Area	6.0225e-002 m^2
Minimum Edge Length	3.1416e-002 m

Figure 3-9 Meshing options and settings.